similar to that of the reflectance changes induced by the same stimuli [28]. Thus, the reflectance changes investigated in this study represented the hemodynamic responses of the retina and optic nerve to the increased retinal neural activity, which are secondary to the activation of the neural activity of the retina. We suggest that the RCs represent the response of neurovascular coupling and TES might stimulate the neurovascular coupling in the retina and optic nerve.

In conclusion, the intensities of the reflectance changes were dependent on the stimulus parameters of TES. The reflectance changes represent changes of the retinal vessels and optic disc, and these results indicate that TES influenced neurovascular coupling, i.e., RGCs and retinal hemodynamics. More experiments are necessary to determine the retinal neurovascular coupling, i.e., the relationship between the activated RGCs and the retinal hemodynamics. However, we conclude that this imaging technique might be a method to investigate the neurovascular coupling.

Author Contributions

Conceived and designed the experiments: T. Morimoto TF. Performed the experiments: T. Morimoto HK T. Miyoshi YH T. Mihashi YK TF. Analyzed the data: T. Morimoto HK YH T. Mihashi. Contributed reagents/materials/analysis tools: T. Morimoto HK T. Miyoshi YH T. Mihashi YK TF. Wrote the paper: T. Morimoto KN TF.

References

1. Potts AM, Inoue J (1968) The electrically evoked response of the visual system (EER). Invest Ophthalmol 7: 269–278.
2. Potts AM, Inoue J (1969) The electrically evoked response of the visual system (EER) II. Effect of adaptation and retinitis pigmentosa. Invest Ophthalmol 8: 605–613.
3. Miyake Y, Yanagida K, Yagasaki K (1980) Clinical application of EER (electrically evoked response). (1) Analysis of EER in normal subjects. Nippon Ganka Gakkai Zasshi 84: 354–360.
4. Fujikado T, Morimoto T, Matsushita K, Shimojo H, Okawa Y, et al. (2006) Effect of transcorneal electrical stimulation in patients with nonarteritic ischemic optic neuropathy or traumatic optic neuropathy. Jpn J Ophthalmol 50 : 266–273.
5. Inomata K, Shinoda K, Ohde H, Tsunoda K, Hanazono G, et al. (2007) Transcorneal electrical stimulation of retina to treat longstanding retinal artery occlusion. Graefes Arch Clin Exp Ophthalmol 245: 1773–1780.
6. Gall C, Fedorov AB, Ernst L, Borrmann A, Sabel BA (2010) Repetitive transorbital alternating current stimulation in optic neuropathy. NeuroRehabilitation 27: 335–341.
7. Schatz A, Röck T, Naycheva L, Willmann G, Wilhelm B, et al. (2011) Transcorneal electrical stimulation for patients with retinitis pigmentosa: a prospective, randomized, sham-controlled exploratory study. Invest Ophthalmol Vis Sci 23: 4485–4496.
8. Delbeke J, Pins D, Michaux G, Wanet-Defalque MC, Parrini S, et al. (2001) Electrical stimulation of anterior visual pathways in retinitis pigmentosa. Invest Ophthalmol Vis Sci 42: 291–297.
9. Morimoto T, Fukui T, Matsushita K, Okawa Y, Shimojyo H, et al. (2006) Evaluation of residual retinal function by pupillary constrictions and phosphenes using transcorneal electrical stimulation in patients with retinal degeneration. Graefes Arch Clin Exp Ophthalmol 244: 1283–1292.
10. Fujikado T, Morimoto T, Kanda H, Kusaka S, Nakauchi K, et al. (2007) Evaluation of phosphenes elicited by extraocular stimulation in normals and by suprachoroidal-transretinal stimulation in patients with retinitis pigmentosa. Graefes Arch Clin Exp Ophthalmol 245: 1411–1419.
11. Naycheva L, Schatz A, Röck T, Willmann G, Messias A, et al. (2012) Phosphene thresholds elicited by transcorneal electrical stimulation in healthy subjects and patients with retinal diseases. Invest Ophthalmol Vis Sci 53: 7440–7448.
12. Shimazu K, Miyake Y, Watanabe S (1999) Retinal ganglion cell response properties in the transcorneal electrically evoked response of the visual system. Vision Res 39: 2251–2260.
13. Shah HA, Montezuma SR, Rizzo JF 3rd (2006) In vivo electrical stimulation of rabbit retina: effect of stimulus duration and electrical field orientation. Exp Eye Res 83: 247–254.
14. Knighton RW (1975) An electrically evoked slow potential of the frog's retina. I. Properties of response. J Neurophysiol.; 38(1): 185–97.
15. Grinvald A, Lieke E, Frostig RD, Gilbert CD, Wiesel TN (1986) Functional architecture of cortex revealed by optical imaging of intrinsic signals. Nature 324: 361–364.
16. Frostig RD, Lieke EE, Ts'o DY, Grinvald A (1990) Cortical functional architecture and local coupling between neuronal activity and the microcirculation revealed by in vivo high-resolution optical imaging of intrinsic signals. Proc Natl Acad Sci USA 87: 6082–6086.
17. Ts'o DY, Frostig RD, Lieke EE, Grinvald A (1990) Functional organization of primate visual cortex revealed by high resolution optical imaging. Science 249: 417–420.
18. Fukuda M, Rajagopalan UM, Homma R, Matsumoto M, Nishizaki M, et al. (2005) Localization of activity-dependent changes in blood volume to submillimeter-scale functional domains in cat visual cortex. Cerebral Cortex 15: 823–833.
19. Cohen LB (1973) Changes in neuron structure during action potential propagation and synaptic transmission. Physiol Rev 53: 373–418.
20. Tsunoda K, Oguchi Y, Hanazono G, Tanifuji M (2004) Mapping cone- and rod- induced retinal responsiveness in macaque retina by optical imaging. Invest Ophthalmol Vis Sci 45: 3820–3826.
21. Abràmoff MD, Kwon YH, Ts'o D, Soliz P, Zimmerman B, et al. (2006) Visual stimulus-induced changes in human near-infrared fundus reflectance. Invest Ophthalmol Vis Sci 47: 715–721.
22. Okawa Y, Fujikado T, Miyoshi T, Sawai H, Kusaka S, et al. (2007) Optical imaging to evaluate retinal activation by electrical currents using suprachoroidal–transretinal stimulation. Invest Ophthalmol Vis Sci 48: 4777–4784.
23. Hanazono G, Tsunoda K, Shinoda K, Tsubota K, Miyake Y, et al. (2007) Intrinsic signal imaging in macaque retina reveals different types of flash-induced light reflectance changes of different origins. Invest Ophthalmol Vis Sci 48: 2903–2912.
24. Inomata K, Tsunoda K, Hanazono G, Kazato Y, Shinoda K, et al. (2008) Distribution of retinal responses evoked by transscleral electrical stimulation detected by intrinsic signal imaging in macaque monkeys. Invest Ophthalmol Vis Sci 49: 2193–2200.
25. Hanazono G, Tsunoda K, Kazato Y, Tsubota K, Tanifuji M (2008) Evaluating neural activity of retinal ganglion cells by flash-evoked intrinsic signal imaging in macaque retina. Invest Ophthalmol Vis Sci 49: 4655–4663.
26. Schallek J, Li H, Kardon R, Kwon Y, Abramoff M, et al. (2009) Stimulus-evoked intrinsic optical signals in the retina: spatial and temporal characteristics. Invest Ophthalmol Vis Sci 50: 4865–4872.
27. Schallek J, Kardon R, Kwon Y, Abramoff M, Soliz P, et al. (2009) Stimulus-evoked intrinsic optical signals in the retina: pharmacologic dissection reveals outer retinal origins. Invest Ophthalmol Vis Sci 50: 4873–4880.
28. Tsunoda K, Hanazono G, Inomata K, Kazato Y, Suzuki W, et al. (2009) Origins of retinal intrinsic signals: a series of experiments on retinas of macaque monkeys. Jpn J Ophthalmol 53: 297–314.
29. Ts'o D, Schallek J, Kwon Y, Kardon R, Abramoff M, et al. (2009) Noninvasive functional imaging of the retina reveals outer retinal and hemodynamic intrinsic optical signal origins. Jpn J Ophthalmol 53: 334–344.
30. Schallek J, Ts'o D (2011) Blood contrast agents enhance intrinsic signals in the retina: evidence for an underlying blood volume component. Invest Ophthalmol Vis Sci 52: 1325–1335.
31. Mihashi T, Okawa Y, Miyoshi T, Kitaguchi Y, Hirohara Y, et al. (2011) Comparing retinal reflectance changes elicited by transcorneal electrical retinal stimulation with those of optic chiasma stimulation in cats. Jpn J Ophthalmol 55: 49–56.
32. Roy CS, Sherrington CS (1890) On the regulation of the blood supply of the brain. J. Physiol 11: 85–108.
33. Riva CE, Logean E, Falsini B (2005) Visually evoked hemodynamical response and assessment of neurovascular coupling in the optic nerve and retina. Prog Retin Eye Res 24: 183–215.
34. Riva CE, Harino S, Shonat RD, Petrig BL (1991) Flicker evoked increase in optic nerve head blood flow in anesthetized cats. Neurosci Lett 128: 291–296.
35. Riva CE, Cranstoun SD, Petrig BL (1996) Effect of decreased ocular perfusion pressure on blood flow and the flicker-induced flow response in the cat optic nerve head. Microvasc Res 52: 258–269.
36. Kurimoto T, Oono S, Oku H, Tagami Y, Kashimoto R, et al. (2010) Transcorneal electrical stimulation increases chorioretinal blood flow in normal human subjects. Clin Ophthalmol 4: 1441–1446.

Clinical Ophthalmology

Dovepress
open access to scientific and medical research

Open Access Full Text Article

ORIGINAL RESEARCH

Comparison of single injection and three monthly injections of intravitreal bevacizumab for macular edema associated with branch retinal vein occlusion

Yuka Ito
Yoshitsugu Saishin
Osamu Sawada
Masashi Kakinoki
Taichiro Miyake
Tomoko Sawada
Hajime Kawamura
Masahito Ohji

Department of Ophthalmology, Shiga University of Medical Science, Otsu, Shiga, Japan

Purpose: Our aim was to compare the 1 year efficacy and safety results of intravitreal bevacizumab (IVB) in two prospective, consecutive groups of patients with macular edema (ME) following branch retinal vein occlusion (BRVO).

Patients and methods: Twenty-five eyes with ME after BRVO received one IVB injection (single-injection group) and 27 eyes received three monthly IVB injections (three-injection group). Both groups were followed monthly for 12 months. The best-corrected visual acuity (BCVA) and the central foveal thickness (CFT) on optical coherence tomography were evaluated before and after treatment. Patients were eligible to receive an IVB injection if the mean CFT increased 100 μm or more or the BCVA decreased 0.1 logarithm of the minimum angle of resolution (logMAR) unit or more compared with values measured on the last visit.

Results: The mean logMAR BCVA and CFT, respectively, improved from 0.56 to 0.33 and from 598 μm to 348 μm in the single-injection group ($P<0.001$) and from 0.55 to 0.26 and from 514 μm to 293 μm in the three-injection group ($P<0.001$). During the study period, the mean total number of injections was significantly smaller in the single-injection group than in the three-injection group (2.1 and 4.3, respectively, $P<0.001$). No serious complications related to the IVB injections developed in either group.

Conclusion: The single-injection group achieved similar visual outcomes for ME secondary to BRVO with fewer injections compared with the three-injection group.

Keywords: branch retinal vein occlusion, bevacizumab, single intravitreal injection, three monthly intravitreal injections

Introduction

Retinal occlusive disorders are second in prevalence after diabetic retinopathy.[1] Macular edema (ME) associated with branch retinal vein occlusion (BRVO) is a common complication.[2] Although a study reported that macular grid-pattern laser photocoagulation improved visual acuity (VA), most patients had limited improvement in VA in other studies.[2–5] Some studies have reported that intravitreal injection of triamcinolone acetonide decreased ME, but this treatment frequently caused adverse effects.[1,2,6,7]

Intravitreal bevacizumab (IVB) injections have been reported to be effective.[8–11] However, IVB injection is an off-label treatment and there are no specific recommendations regarding the frequency of injection for effective long-term results.

We studied two prospective, consecutive groups of patients with ME following BRVO. One group received a single IVB injection, the other received three monthly IVB injections, and the 1 year efficacy and safety results were compared in the two groups.

Correspondence: Yoshitsugu Saishin
Department of Ophthalmology, Shiga University of Medical Science, Seta-Tsukinowacho, Otsu, Shiga 520-2192, Japan
Tel +81 77 548 2276
Fax +81 77 548 2279
Email saishin@belle.shiga-med.ac.jp

submit your manuscript | www.dovepress.com
Dovepress
http://dx.doi.org/10.2147/OPTH.S76261

Patients and methods

Inclusion criteria

Patients with ME after BRVO were included. Patients had a central foveal thickness (CFT) exceeding 300 μm on optical coherence tomography (OCT; Cirrus HD-OCT, Carl Zeiss Meditec AG, Jena, Germany) and a decimal VA of 0.5 or worse.

Exclusion criteria

Eyes with glaucoma, diabetic retinopathy, and inflammatory disease were excluded. Patients with a recent history of stroke or myocardial infarction, unstable angina pectoris, uncontrolled hypertension, uncompensated renal insufficiency, pregnancy, prior anti-vascular endothelial growth factor (VEGF) treatment or allergy to bevacizumab were also excluded.

Re-injection criteria

Patients were eligible to receive an IVB injection if there was an increase in the mean CFT of 100 μm or more or a decrease in the BCVA of 0.1 logarithm of the minimum angle of resolution (logMAR) unit or more compared with values measured on the last visit.

Single-injection group

We prospectively analyzed 25 consecutive eyes of 25 patients (nine males and 16 females) with ME following BRVO who were enrolled from August 2007 to March 2009 at the Shiga University of Medical Science Hospital. The Institutional Review Board of the hospital approved the study protocol. Patients received one IVB injection at baseline and no additional treatments were performed within 3 months of the initial injection (month 1 and month 2). IVB was administered as needed if the pre-specified criteria were met during months 3 to 11 (referred to as the pro re nata [PRN] period). Four patients received prior treatment with photocoagulation (three patients) or posterior sub-tenon injection of triamcinolone acetonide (one patient) more than 9 months prior to the first IVB injection.

Three-injection group

We prospectively consecutively studied 27 eyes of 27 patients (15 males and 12 females) with ME after BRVO who were enrolled from December 2009 to November 2010 at the Shiga University of Medical Science Hospital. The Institutional Review Board of the Shiga University of Medical Science Hospital approved the study protocol. Patients received three monthly IVB injections (day 0 – month 2). IVB was then administered as needed if pre-specified criteria were met during the PRN period. Two patients received prior treatment with photocoagulation (one patient) or posterior sub-tenon injection of triamcinolone acetonide (one patient) more than 5 months prior to the first IVB injection.

Study visits and assessments

Patients were examined at baseline (day 0), week 1, and then monthly from months 1 to 12. At each visit, patients underwent a complete ocular examination. The BCVA was expressed as decimal VA using a Landolt C chart and converted to logMAR VA for analysis. The CFT was measured using the macular cube 512×128 mode protocol and defined as the central area within a diameter of 1 mm on Cirrus HD-OCT images.

Statistical analysis

Data were analyzed using SPSS II for Windows (SPSS Inc., Chicago, IL, USA). Differences in the logMAR BCVA and CFT between baseline and 12 months after the first injection were analyzed using a paired samples *t*-test. Differences in the changes in the logMAR BCVA and CFT between the two treatment groups were analyzed using a two-sample Student's *t*-test. A *P*-value less than 0.05 was considered to be statistically significant.

A chi-square test was used to compare the difference in percentage of patients who gained 0.3 logMAR units or more in BCVA between the two groups.

Results

Baseline characteristics

The baseline characteristics are shown in Table 1. The mean (± standard deviation) age was 69.3±7.8 years (range 55–81) in the single-injection group and 68.0±10.7 years (range 44–88) in the three-injection group. There were no significant differences between the groups in gender, age, BCVA, or CFT.

Duration of BRVO before the treatment

There was no significant difference in mean interval between the onset of BRVO and the first intravitreal injection of bevacizumab (3.57±2.87 months [range 1–11] in the single-injection group versus (vs) 3.73±3.03 months [range 1–12] in the three-injection group; P=0.85).

VA

The mean logMAR BCVA values are shown in Figure 1. There was no significant difference in the mean logMAR

Table 1 Baseline patient characteristics in the two treatment groups

Characteristic	Three IVB group (n=27)	Single IVB group (n=25)
No patients	27	25
Female/male (eyes)	12/15	16/9
Age (years, mean ± SD)	68.0±10.7	69.32±7.8
BCVA (logMAR, mean ± SD)	0.55±0.24	0.56±0.22
CFT (μm, mean ± SD)	514±172	598±186

Abbreviations: IVB, intravitreal bevacizumab; BCVA, best-corrected visual acuity; CFT, central foveal thickness; logMAR, logarithm of the minimum angle of resolution; SD, standard deviation.

BCVA at baseline (0.56±0.22 [range 0.30–1.15] in the single-injection group vs 0.55±0.24 [range 0.30–1.05] in the three-injection group; P=0.84). In the single-injection group, the mean logMAR BCVA improved from 0.56±0.22 (range 0.30–1.15) at baseline to 0.47±0.26 (range 0–1.05), 0.42±0.33 (range 0–1.15), 0.39±0.27 (range 0.05–1.05), and 0.33±0.29 (range, −0.18–1.05) at months 1, 3, 6, and 12, respectively, and significantly from 0.56 at baseline to 0.33 at month 12 (P<0.001).

In the three-injection group, the mean baseline logMAR BCVA improved from 0.55±0.24 (range 0.30–1.05) to 0.40±0.24 (range 0–1.00), 0.32±0.22 (range −0.07–0.82), 0.30±0.22 (range 0–0.70) and 0.26±0.25 (range −0.18–0.70) at months 1, 3, 6, and 12, respectively, and significantly from 0.55 at baseline to 0.26 at month 12 (P<0.001). The mean logMAR BCVA did not differ significantly at month 12 between the two groups (P=0.389).

The BCVA improved by 0.3 logMAR units or more at month 12 in nine (36%) eyes, remained stable in 14 (56%) eyes, and worsened by 0.3 logMAR units or more in two (8%) eyes in the single-injection group, and improved by 0.3 logMAR units or more at month 12 in 16 (59%) eyes, remained stable in ten (37%) eyes, and worsened by 0.3 logMAR units or more in one (4%) eye in the three-injection group. There was no between-group difference in the percentage of eyes with improved BCVA (P=0.093) or in the percentage of eyes with worsened logMAR BCVA (P=0.603).

CFT

The mean CFT is shown in Figure 2. In the single-injection group, the mean ± standard deviation CFT decreased from 598±186 μm at baseline to 347±133, 476±139, 384±141, and 348±134 μm at months 1, 3, 6, and 12, respectively, and decreased significantly (P<0.001) from 598±186 μm at baseline to 348±134 μm at month 12. In the three-injection group, the mean CFT decreased significantly (P<0.001) from 514±172 μm at baseline to 277±57, 256±65, 322±114, and 293±102 μm at months 1, 3, 6, and 12, respectively. The mean CFT at month 12 did not differ significantly between the two groups (P=0.101).

Number of additional injections

During the PRN period, additional injections were required in 19 (76%) of 25 eyes in the single-injection group (one injection in eleven eyes, two injections in seven eyes, and three injections in one eye) and 16 (59%) of 27 eyes in the three-injection group (one injection in four eyes, two injections in seven eyes, three injections in three eyes, four injections in one eye, and five injections in one eye). The mean number of additional injections was 1.1±0.8 in the single-injection

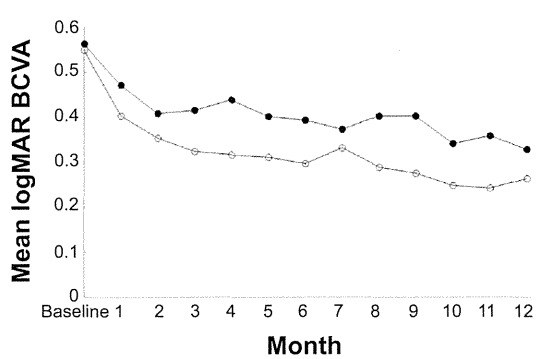

Figure 1 The change in the mean logarithm of the minimum angle of resolution best-corrected visual acuity (logMAR BCVA) from baseline to month 12.
Notes: In the one-injection group (solid circles), the mean logMAR BCVA improved slightly from 0.56 at baseline to 0.47 at month 1 (P=0.04) and improved significantly to 0.33 at month 12 (P<0.001). In the three-injection group (open circles), the mean logMAR BCVA improved further to 0.40 at month 1 (P<0.001) and improved significantly from 0.55 at baseline to 0.26 at month 12 (P<0.001). There was no significant between-group difference in the mean logMAR BCVA at month 12 (P=0.389).

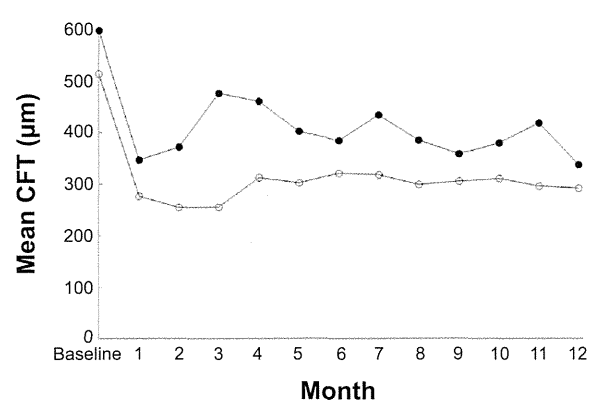

Figure 2 The mean change in central foveal thickness (CFT) from baseline to month 12.
Notes: The mean CFT decreased significantly from 598±186 μm at baseline to 348±134 μm at month 12 in the one-injection group (solid circles; P<0.001) and from 514±172 μm at baseline to 293±102 μm at month 12 in the three-injection group (open circles; P<0.001). There was no significant between-group difference in the mean CFT at month 12 (P=0.101).

group and 1.3±1.4 in the three-injection group. The number of additional injections did not differ significantly (P=0.507) between the two groups.

During the study period, the mean total number of injections was significantly smaller in the single-injection group than in the three-injection group (2.1±0.8 vs 4.3±1.4; P<0.001).

Complications

No serious complications related to the IVB injections developed in either group.

Discussion

Previous studies have reported the efficacy of IVB for ME due to BRVO. However, few studies have reported the long-term efficacy of three monthly IVB injections and to our best knowledge, no studies have reported the results of treatment with single IVB injections and three monthly IVB injections in two prospective, consecutive groups of patients with ME following BRVO and compared the 1 year efficacy and safety results between these groups. A total of 52 patients were enrolled in the study, ie, 25 consecutive eyes of 25 patients initially treated with one IVB injection followed by PRN treatment and 27 consecutive eyes of 27 patients initially treated with three monthly IVB injections followed by PRN treatment.

The mean logMAR BCVA improved significantly from 0.56 at baseline to 0.33 at month 12 in the single injection group (P<0.001) and from 0.55 at baseline to 0.26 at month 12 in the three-injection group (P<0.001). The current results were similar to those of previous studies (Table 2).[12–15] Comparing the results among different studies is difficult because of the variations in inclusion criteria and different retreatment criteria. In the current study, 1 year efficacy and safety results were compared between two groups of patients with ME after BRVO (a single IVB injection group and three monthly IVB injection group). The groups were comparable because we prospectively used the same inclusion criteria, the same retreatment criteria, and the same follow-up schedule except for the loading phase. Patients in the two groups were not randomized. However, we believe that the likelihood of sample selection bias was small because consecutive patients in the single-injection group were enrolled from August 2007 to March 2009, and consecutive patients in the three-injection group were enrolled from December 2009 to November 2010. After comparing the results, there was no significant (P=0.389) difference between the two groups regarding improvement in the logMAR BCVA.

Consistent with previous findings (Table 2),[12–15] we found that the mean CFT decreased significantly from 598 μm at baseline to 348 μm at month 12 in the single-injection group (P<0.001) and from 514 μm at baseline to 293 μm at month 12 in the three-injection group (P<0.001). There was no significant (P=0.101) between-group difference in CFT improvement.

Krohne et al reported that drug elimination from the aqueous humor closely parallels that from the vitreous and concluded that the aqueous half-life of 1.5 mg of intravitreally injected bevacizumab in humans is 9.82 days.[16] Miyake et al reported that the half-life of 1.25 mg of intravitreally injected bevacizumab in macaque eyes is 2.8 days in the aqueous humor.[17] The half-life of bevacizumab is therefore short and retreatment is often required.[16–18] In the current study, the average number of additional injections was 1.1 in the single-injection group, and re-injections were performed in 19 (76%) eyes during the PRN period. In the three-injection group, the average number of additional injections was 1.3, and re-injections were performed in 16 (59%) eyes during the PRN period. Comparison of results of IVB injection at 12 months between previous studies and the current study is shown in Table 2.

It is difficult to compare the mean number of additional injections among different studies because of inter-study

Table 2 Comparison of results of intravitreal injection of bevacizumab at 12 months between previous studies and the current study

Study	Current study single injection	Jaissle et al[12]	Kondo et al[13]	Current study three monthly injections	Demir et al[15]
Eyes	25	23	50	27	33
Injections	Single	Single	Single	Three monthly	Three monthly
Baseline BCVA	0.56	0.50	0.53	0.55	0.66
BCVA at 12 months	0.33	0.20	0.26	0.26	0.22
Baseline CFT	598	395	523	514	494
CFT at 12 months	348	255	305	293	262
Additional injections	1.1	2.4	1.0	1.3	2.3

Abbreviations: BCVA, best-corrected visual acuity; CFT, central foveal thickness.

variation in inclusion criteria and retreatment criteria. In the current study, the mean number of additional injections was compared between the single-injection group and the three-injection group because the same inclusion and retreatment criteria were used prospectively, and no significant between-group difference in the number of additional injections was shown (P=0.507).

The mean total number of injections was smaller in the single-injection group than the three-injection group (2.1±0.8 vs 4.3±1.4, respectively) because the mean number of additional injections was similar between the two groups. No serious complications developed in either group. Therefore, the single injection protocol was safer and less invasive than the three-injection one.

The mean CFT in the single-injection group increased at months 2 and 3 and retreatment guidelines prohibited additional injections. There was no significant difference in the logMAR BCVA between the two groups at months 2 and 3 (P=0.403 and P=0.244, respectively). Increases in the CFT in the short term may not have an immediate effect on BCVA, whereas increases in the CFT in the long term may result in worsening of the BCVA.[19]

The absence of a significant between-group difference in the mean CFT and the logMAR BCVA at month 12 in patients with ME after BRVO indicated that one IVB injection followed by PRN treatment had similar effectiveness to three monthly IVB injections followed by PRN treatment in improving BCVA and CFT. Furthermore, the total number of injections was smaller in the single-injection group than in the three-injection group.

No complications occurred in our two study groups, but severe side effects occurred in other studies. Minimizing the total number of injections reduces the risk of complications associated with IVB.

Although circulating VEGF protects the integrity and patency of vessels, prolonged anti-VEGF treatment can increase the risk of thromboembolic events,[20–22] and reduced number of injections can lower the risk of serious adverse events.

Notably, one limitation of our study was the relatively small number of patients with available imaging, possibly preventing our analysis from reaching statistical significance.

We showed that similar visual outcomes for ME secondary to BRVO may be achieved with fewer injections when one IVB injection is followed by PRN treatment rather than when three IVB injections are followed by PRN treatment; however, a prospective, double-masked, randomized study with a large number of patients is warranted.

Disclosure

Supported in part by a grant from the Ministry of Education, Culture, Sports, Science and Technology of Japan (#24592668). The authors have no conflicts of interest to disclose.

References

1. Cakir M, Dogan M, Bayraktar Z, et al. Efficacy of intravitreal triamcinolone for the treatment of macular edema secondary to branch retinal vein occlusion in eyes with or without grid laser photocoagulation. *Retina*. 2008;28(3):465–472.
2. Rehak J, Rehak M. Branch retinal vein occlusion: Pathogenesis, visual prognosis, and treatment modalities. *Curr Eye Res*. 2008;33(2):111–131.
3. No authors listed. Argon laser photocoagulation for macular edema in branch vein occlusion. The branch vein occlusion study group. *Am J Ophthalmol*. 1984;98(3):271–282.
4. Battaglia Parodi M, Saviano S, Ravalico G. Grid laser treatment in macular branch retinal vein occlusion. *Graefes Arch Clin Exp Ophthalmol*. 1999;237(12):1024–1027.
5. Battaglia Parodi M, Saviano S, Bergamini L, Ravalico G. Grid laser treatment of macular edema in macular branch retinal vein occlusion. *Doc Ophthalmol*. 1999;97(3–4):427–431.
6. Cekic O, Chang S, Tseng JJ, et al. Intravitreal triamcinolone injection for treatment of macular edema secondary to branch retinal vein occlusion. *Retina*. 2005;25(7):851–855.
7. Higashiyama T, Sawada O, Kakinoki M, Sawada T, Kawamura H, Ohji M. Prospective comparisons of intravitreal injections of triamcinolone acetonide and bevacizumab for macular oedema due to branch retinal vein occlusion. *Acta Ophthalmol*. 2013;91(4):318–324.
8. Rabena MD, Pieramici DJ, Castellarin AA, Nasir MA, Avery RL. Intravitreal bevacizumab (avastin) in the treatment of macular edema secondary to branch retinal vein occlusion. *Retina*. 2007;27(4):419–425.
9. Gunduz K, Bakri SJ. Intravitreal bevacizumab for macular oedema secondary to branch retinal vein occlusion. *Eye (Lond)*. 2008;22(9):1168–1171.
10. Moradian S, Faghihi H, Sadeghi B, et al. Intravitreal bevacizumab vs Sham treatment in acute branch retinal vein occlusion with macular edema: Results at 3 months (report 1). *Graefes Arch Clin Exp Ophthalmol*. 2011;249(2):193–200.
11. Yunoki T, Miyakoshi A, Nakamura T, Fujita K, Fuchizawa C, Hayashi A. Treatment of macular edema due to branch retinal vein occlusion with single or multiple intravitreal injections of bevacizumab. *Jpn J Ophthalmol*. 2012;56(2):159–164.
12. Jaissle GB, Leitritz M, Gelisken F, Ziemssen F, Bartz-Schmidt KU, Szurman P. One-year results after intravitreal bevacizumab therapy for macular edema secondary to branch retinal vein occlusion. *Graefes Arch Clin Exp Ophthalmol*. 2009;247(1):27–33.
13. Kondo M, Kondo N, Ito Y, et al. Intravitreal injection of bevacizumab for macular edema secondary to branch retinal vein occlusion: Results after 12 months and multiple regression analysis. *Retina*. 2009; 29(9):1242–1248.
14. Byun YJ, Roh MI, Lee SC, Koh HJ. Intravitreal triamcinolone acetonide versus bevacizumab therapy for macular edema associated with branch retinal vein occlusion. *Graefes Arch Clin Exp Ophthalmol*. 2010;248(7):963–971.
15. Demir M, Oba E, Gulkilik G, Odabasi M, Ozdal E. Intravitreal bevacizumab for macular edema due to branch retinal vein occlusion: 12-month results. *Clin Ophthalmol*. 2011;5:745–749.
16. Krohne TU, Eter N, Holz FG, Meyer CH. Intraocular pharmacokinetics of bevacizumab after a single intravitreal injection in humans. *Am J Ophthalmol*. 2008;146(4):508–512.
17. Miyake T, Sawada O, Kakinoki M, et al. Pharmacokinetics of bevacizumab and its effect on vascular endothelial growth factor after intravitreal injection of bevacizumab in macaque eyes. *Invest Ophthalmol Vis Sci*. 2010;51(3):1606–1608.

18. Bakri SJ, Snyder MR, Reid JM, Pulido JS, Singh RJ. Pharmacokinetics of intravitreal bevacizumab (avastin). *Ophthalmology*. 2007;114(5):855–859.
19. Heier JS, Brown DM, Chong V, et al. Intravitreal aflibercept (vegf trap-eye) in wet age-related macular degeneration. *Ophthalmology*. 2012;119(2):2537–2548.
20. Costagliola C, Agnifili L, Arcidiacono B, et al. Systemic thromboembolic adverse events in patients treated with intravitreal anti-VEGF drugs for neovascular age-related macular degeneration. *Expert Opin Biol Ther*. 2012;12(10):1299–1313.
21. Semeraro F, Morescalchi F, Duse S, Gambicorti E, Romano MR, Costagliola C. Systemic thromboembolic adverse events in patients treated with intravitreal anti-VEGF drugs for neovascular age-related macular degeneration: an overview. *Expert Opin Drug Saf*. 2014;13(6):785–802.
22. Schmid MK, Bachmann LM, Fäs L, Kessels AG, Job OM, Thiel MA. Efficacy and adverse events of aflibercept, ranibizumab and bevacizumab in age-related macular degeneration: a trade-off analysis. *Br J Ophthalmol*. Epub 2014 Jun 11.

Retina

Effect of Vitrectomy on Aqueous VEGF Concentration and Pharmacokinetics of Bevacizumab in Macaque Monkeys

Masashi Kakinoki, Osamu Sawada, Tomoko Sawada, Yoshitsugu Saishin, Hajime Kawamura, and Masahito Ohji

Purpose. To evaluate the effect of vitrectomy on the concentration of vascular endothelial growth factor (VEGF) and the pharmacokinetics of intravitreally injected bevacizumab in the aqueous humor in cynomolgus macaques.

Methods. Pars plana lensectomy and a standard three-port vitrectomy were performed in one eye each of six macaques. After a minimal 12-week healing period, the vitrectomized eyes received an intravitreal injection of bevacizumab (1.25 mg/50 μL). Aqueous humor and venous blood samples were obtained from the macaques just before vitrectomy, just before injection of bevacizumab, on days 1, 3, and 7, and during weeks 2, 4, 6, and 8 after the injection. The bevacizumab and VEGF concentrations were measured by using enzyme-linked immunosorbent assay.

Results. The VEGF concentrations in the aqueous humor ranged from 52.6 to 113.9 pg/mL (mean ± standard deviation [SD], 81.7 ± 27.0 pg/mL) before vitrectomy and 20.7 to 72.7 pg/mL (mean ± SD, 51.4 ± 20.5 pg/mL) 3 months after vitrectomy, a difference that reached significance ($P = 0.03$). The aqueous VEGF concentrations decreased to less than 9.0 pg/mL, the lower limit of detection, in all eyes between 1 and 7 days after injection of bevacizumab. The mean half-life of 1.25 mg intravitreally injected bevacizumab was 1.5 ± 0.6 days (range, 1.0–2.4 days) in the aqueous humor.

Conclusions. The VEGF concentration in the aqueous humor decreased and the half-life of the intravitreally injected bevacizumab was shorter in vitrectomized eyes. (*Invest Ophthalmol Vis Sci.* 2012;53:5877–5880) DOI:10.1167/iovs.12-10164

Bevacizumab (Avastin; Genentech, South San Francisco, CA), a full-length humanized monoclonal antibody to all isoforms of vascular endothelial growth factor (VEGF), received US Food and Drug Administration approval for intravenous treatment of metastatic colorectal cancer in 2004. Intravitreal injection of bevacizumab has been used widely to treat various ocular diseases including age-related macular degeneration, retinal vein occlusion, and proliferative diabetic retinopathy.[1–8] Although numerous reports on the efficacy of intravitreal injections of bevacizumab have been published, few studies have reported on the pharmacokinetics of the drug. We have previously reported that intravitreal injection of bevacizumab decreases the VEGF concentration in normal eyes for approximately 4 weeks but has no or a minimal effect on the untreated fellow eyes in macaques, and the half-life of 1.25 mg intravitreally injected bevacizumab is 2.8 ± 0.6 days in the aqueous humor.[9] To the best of our knowledge, no studies have compared the VEGF concentration between vitrectomized and nonvitrectomized eyes of cynomolgus macaques. To evaluate the effect of vitrectomy on the VEGF concentration and the pharmacokinetics of intravitreally injected bevacizumab in the aqueous humor in cynomolgus macaques, we measured the VEGF and bevacizumab concentrations over time in the aqueous humor of the injected and uninjected eyes before vitrectomy and before and after intravitreal injection of bevacizumab in vitrectomized eyes of cynomolgus macaques.

Methods

All treatments were performed in accordance with the Association for Research in Vision and Ophthalmology Statement for the Use of Animals in Ophthalmic and Vision Research, and the Animal Experimentation Committee of Shiga University of Medical Science approved the animal research protocol. Six male cynomolgus macaques, aged 7 to 10 years and weighing 4.5 to 8.5 kg, were anesthetized with 5 mg/kg intramuscular ketamine hydrochloride, 1 mg/kg intramuscular xylazine hydrochloride, and 1% isoflurane. The pupils were dilated with 1 drop of 10% phenylephrine hydrochloride ophthalmic solution. The surgical eye was irrigated with 0.02% chlorhexidine gluconate and anesthetized with 1 drop of 4% xylocaine for additional anesthesia. Aqueous humor samples (150 μL) were obtained from the macaques just before vitrectomy. After a limbal-based conjunctival incision was made, three 20-gauge ports were made on the sclera 3.5 mm from the limbus. A standard three-port vitrectomy and pars plana lensectomy was performed in one eye each of six macaques. We did not intend to create posterior vitreous detachment. The monkeys recovered from the postoperative inflammation for a minimum of 12 weeks before entering the pharmacokinetic study. No signs of infections or inflammation were found at 12 weeks after the vitrectomy, and no retinal detachments developed.

Bevacizumab (1.25 mg/50 μL) was injected with a 29-gauge needle into the vitreous cavity of the vitrectomized eye of each macaque after the recovery period. The fellow eyes did not receive an intravitreal injection and served as controls. Both aqueous humor samples (150 μL) and venous blood samples (2 mL) were obtained from the macaques just before the injection and 1, 3, and 7 days and 2, 4, 6, and 8 weeks after the injection. The samples were stored in a freezer at −80°C until analysis.

From the Department of Ophthalmology, Shiga University of Medical Science, Otsu, Japan.

Supported in part by a grant from the Ministry of Education, Culture, Sports, Science and Technology of Japan (18591915) and a grant from the Ministry of Health, Labour and Welfare. The authors have no proprietary interest in any aspect of this report.

Submitted for publication May 8, 2012; revised June 24, 2012; accepted July 22, 2012.

Disclosure: **M. Kakinoki**, None; **O. Sawada**, None; **T. Sawada**, None; **Y. Saishin**, None; **H. Kawamura**, None; **M. Ohji**, None

Corresponding author: Masashi Kakinoki, Department of Ophthalmology, Shiga University of Medical Science, Seta-tsukino-wacho, 520-2192, Otsu, Japan; kakinoki@belle.shiga-med.ac.jp.

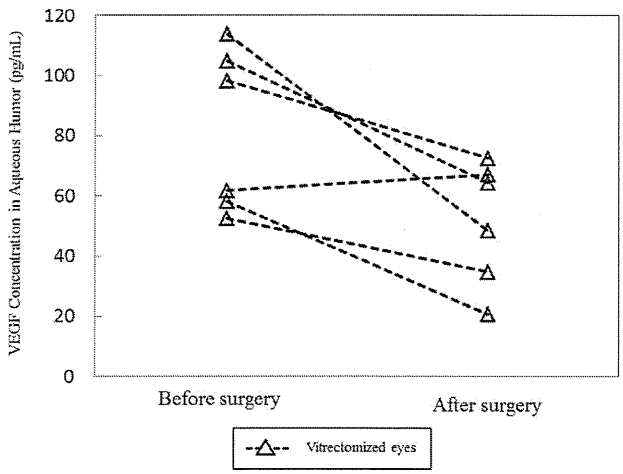

FIGURE 1. Pre- and postoperative VEGF concentrations in the aqueous humor of vitrectomized eyes.

Measurement of VEGF

The VEGF concentrations in the aqueous humor were measured by using a Quantikine Human VEGF Immunoassay (R&D Systems, Minneapolis, MN) according to the manufacturer's instructions. The limit of the detectable VEGF concentration was 9.0 pg/mL. VEGF concentration less than the lower limit of detection was considered as 0 in the calculation for mean.

Measurement of Bevacizumab

The bevacizumab concentration was measured by using a slightly modified enzyme-linked immunosorbent assay as previously described.[10] Ninety-six well plates were coated with recombinant human VEGF165 (R&D Systems) at a concentration of 1.0 μg/mL overnight at 4°C (100 μL/well). After washing three times with phosphate-buffered saline (PBS) containing 0.05% Tween-20, the wells were blocked with 3% bovine serum albumin (BSA)/PBS overnight at 4°C (200 μL/well). The wells then were washed five times with PBS containing 0.05% Tween-20 and stored dry at 4°C for later use. Aqueous humor or serum diluted in 0.1% BSA/PBS was added to the plates overnight at 4°C (50 μL/well). Bevacizumab was detected by horseradish peroxidase–goat anti-human IgG (H+L) conjugate (Invitrogen Corporation, Carlsbad, CA) with a concentration of 1 μg/mL after a 3-hour incubation period at room temperature. After five washes, color development was performed with 100 μL 3,3′,5,5′-tetramethyl benzidine substrate, and

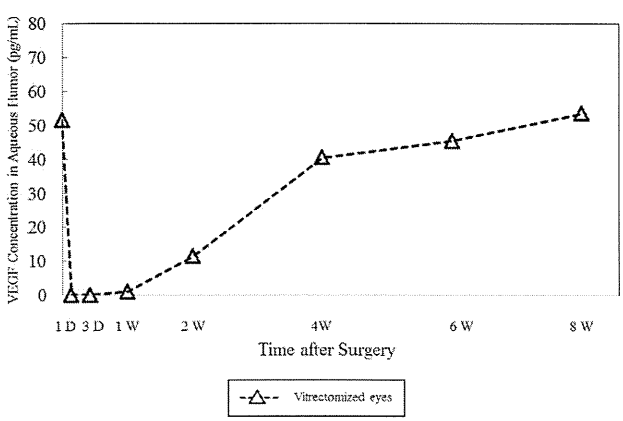

FIGURE 2. VEGF concentrations in the aqueous humor of vitrectomized eye at various time points after surgery. D, days; W, weeks.

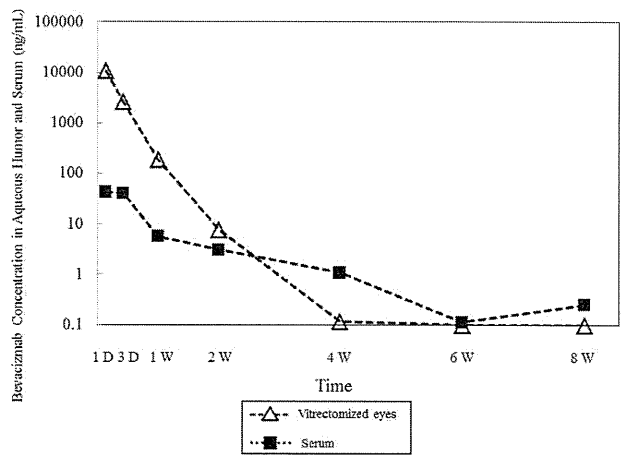

FIGURE 3. Bevacizumab concentrations in the aqueous humor of vitrectomized eye and serum at various time points after surgery.

the reaction was stopped by adding 1 M hydrogen chloride (100 μL). The optical density was measured at 450 nm with correction at 570 nm. A standard curve was prepared with bevacizumab ranging from 7.8 to 1000 pg/mL.

Statistical Analysis

All statistical analyses were carried out by using PASW Statistics 18 (SPSS Japan, Tokyo, Japan).

RESULTS

The VEGF concentrations in the aqueous humor of the study eyes ranged from 52.6 to 113.9 pg/mL (mean ± standard deviation [SD], 81.7 ± 27.0 pg/mL) before vitrectomy and from 20.7 to 72.7 pg/mL (mean ± SD, 51.4 ± 20.5 pg/mL) 3 months postoperatively (Figs. 1, 2). The aqueous VEGF concentrations decreased significantly ($P < 0.03$) in the six vitrectomized eyes. One day after the injection of bevacizumab, the VEGF concentrations in the aqueous humor decreased to less than 9.0 pg/mL, the lower limit of detection in all injected eyes. The concentration below the lower limit was maintained for 1 week in all eyes. At 2 weeks, the VEGF concentration remained below the lower limit of detection in two eyes and returned to a detectable level in four eyes. At 4 weeks, the VEGF concentrations in the aqueous humor of the injected eyes ranged from 17.0 to 93.7 pg/mL (mean, 40.4 ± 28.4 pg/mL). The VEGF concentrations in the aqueous humor of the fellow uninjected eyes ranged from 43.4 to 169.5 pg/mL (mean, 104.6 ± 57.3 pg/mL) before the intravitreal injection and did not change after the injection.

Bevacizumab concentrations in the aqueous humor of the injected eyes peaked at 10.8 ± 6.4 μg/mL (10,800 ± 6400 ng/mL) the day after the injection and declined gradually (Fig. 3). Bevacizumab was not detected in the untreated eyes. The half-life of 1.25 mg intravitreally injected bevacizumab was 1.5 ± 0.6 days (range, 1.0–2.4 days) in the aqueous humor.

A maximal bevacizumab serum concentration of 42.2 ± 34.0 ng/mL was achieved 1 day after the injection and then declined gradually. However, the reduction rate was much less than that in the aqueous humor of the vitrectomized eyes and higher than that in the aqueous humor in the treated eyes at 4 weeks and thereafter. The bevacizumab concentration in the serum 8 weeks after the injection was 0.25 ± 0.16 ng/mL. The half-life of bevacizumab was 5.9 ± 2.0 days (range, 3.0–8.3

days) in the serum. No complications, such as uveitis or endophthalmitis, developed after bevacizumab was injected.

Discussion

In the current study, the VEGF concentrations in the aqueous humor ranged from 52.6 to 113.9 pg/mL (mean ± SD, 81.7 ± 27.0 pg/mL) before the vitrectomy and 20.7 to 72.7 pg/mL (mean ± SD, 51.4 ± 20.5 pg/mL) 3 months after vitrectomy. The aqueous VEGF concentration decreased significantly ($P < 0.03$) in the six vitrectomized eyes. There are several possible explanations for the reduced VEGF concentration in the vitrectomized eyes. The VEGF concentration in the aqueous humor of normal eyes returned to a detectable level 4 weeks after the bevacizumab injection.[9] Therefore, removal of VEGF from the vitreous cannot explain the reduced VEGF concentration 3 months after vitrectomy. Another possible explanation is rapid clearance of VEGF from the vitreous.[11–13] VEGF produced by retina may be more rapidly cleared from the vitrectomized eyes than from the normal eyes, as intravitreally injected drugs have been reported to be cleared more rapidly in vitrectomized eyes. The concentration of aqueous VEGF in the vitrectomized eyes did not decrease because of temporary removal of VEGF but because of the conditions in the vitreous.

Pars plana vitrectomy (PPV) reduces the macular thickness of eyes with diabetic macular edema (DME).[14–16] Yamamoto et al.,[14] who reported the results after PPV was performed in 65 eyes of 63 patients with DME, have found that the postoperative foveal retinal thickness at the final visit is significantly thinner than the preoperative foveal retinal thickness. The authors have suggested that the high oxygen concentrations supplied by the ciliary body cause retinal vasoconstriction and reduce retinal thickness after vitrectomy. Yanyali et al.,[15] who reported the results of PPV with removal of the internal limiting membrane (ILM) in 27 eyes of 27 patients with DME, have found that the mean foveal thickness decreases significantly. They have suggested that removing the ILM might have a beneficial effect in DME by removing tangential traction exerted by the ILM and residual cortical vitreous. Hartly et al.,[16] also have reported that PPV with removal of the ILM results in decreased retinal thickness in patients with DME. In addition to those reports, a decrease in the VEGF concentration in the aqueous humor in vitrectomized eyes might cause a reduction of the foveal thickness in patients with DME.

In the current study, the VEGF concentration in the aqueous humor of the vitrectomized eyes fell below the lower limit of detection after the bevacizumab injection and remained low for approximately 2 weeks. The VEGF concentration returned to a detectable level after 2 to 4 weeks in vitrectomized eyes. Faster clearance of the bevacizumab in the vitrectomized eye might result in a shorter period of drug effectiveness.

The current study showed that the half-life of intravitreally injected bevacizumab was 1.5 ± 0.6 days in the vitrectomized eye. We previously have reported that the half-life of intravitreally injected bevacizumab in normal eyes of macaques is 2.8 ± 0.6 days ($n = 3$; range, 2.3–3.5 days). The half-life of the intravitreally injected bevacizumab in the vitrectomized eyes decreased by 54% compared with the nonvitrectomized normal eyes. Recently, intravitreal bevacizumab injections are being administered more and more often to treat some ophthalmic diseases. However, the precise difference in the intravitreal bevacizumab concentrations between vitrectomized and nonvitrectomized eyes is unknown. Some intravitreal drugs clear more rapidly in vitrectomized eyes than in nonvitrectomized eyes.[11–13] Doft et al.[11] have studied ocular clearance after 10-μg intravitreal injections of amphotericin B in vitrectomized and nonvitrectomized rabbit models and report half-lives of 1.4 days and 9.1 days, respectively. Chin et al.[12] have studied the difference in the clearance of 0.3-mg intravitreal injections of triamcinolone acetonide between vitrectomized and nonvitrectomized rabbit models and report half-lives of 1.57 days and 2.89 days, respectively. Lee et al.[13] also have studied the differences in clearance of 500 ng intravitreal human $VEGF_{165}$ between vitrectomized and nonvitrectomized rabbit models and report the half-lives of 12.5 minutes and 2.46 hours, respectively. The duration of the decreased concentration of VEGF after intravitreal injection of bevacizumab was shorter in vitrectomized eyes than in nonvitrectomized eyes probably because of the shorter half-life of bevacizumab. Faster clearance of intravitreal bevacizumab should be considered when planning intravitreal injections of bevacizumab in vitrectomized eyes.

In conclusion, the aqueous VEGF concentration decreased in vitrectomized eyes, and the half-life of intravitreal injections of bevacizumab was shorter in vitrectomized eye than in nonvitrectomized eyes. Careful attention should be paid to the duration of the effectiveness of intravitreal injections of bevacizumab in vitrectomized eyes.

References

1. Michels S, Rosenfeld PJ, Puliafito CA, Marcus EN, Venkatraman AS. Systemic bevacizumab (Avastin) therapy for neovascular age-related macular degeneration: twelve-week results of an uncontrolled open-label clinical study. *Ophthalmology.* 2005; 112:1035–1047.
2. Moshfeghi AA, Rosenfeld PJ, Puliafito CA, et al. Systemic bevacizumab (Avastin) therapy for neovascular age-related macular degeneration: twenty-four-week results of an uncontrolled open-label clinical study. *Ophthalmology.* 2006;113: 2002–2011.
3. Avery RL, Pearlman J, Pieramici DJ, et al. Intravitreal bevacizumab (Avastin) in the treatment of proliferative diabetic retinopathy. *Ophthalmology.* 2006;113:1695–1705.
4. Spaide RF, Fisher YL. Intravitreal bevacizumab (Avastin) treatment of proliferative diabetic retinopathy complicated by vitreous hemorrhage. *Retina.* 2006;26:275–278.
5. Sawada O, Kawamura H, Kakinoki M, Ohji M. Vascular endothelial growth factor in aqueous humor before and after intravitreal injection of bevacizumab in eyes with diabetic retinopathy. *Arch Ophthalmol.* 2007;125:1363–1366.
6. Spaide RF, Laud K, Fine HF, et al. Intravitreal bevacizumab treatment of choroidal neovascularization secondary to age-related macular degeneration. *Retina.* 2006;26:383–390.
7. Rosenfeld PJ, Fung AE, Puliafito CA. Optical coherence tomography findings after an intravitreal injection of bevacizumab (Avastin) for macular edema from central retinal vein occlusion. *Ophthalmic Surg Lasers Imaging.* 2005;36:336–339.
8. Iturralde D, Spaide RF, Meyerle CB, et al. Intravitreal bevacizumab (Avastin) treatment of macular edema in central retinal vein occlusion: a short-term study. *Retina.* 2006;26: 279–284.
9. Miyake T, Sawada O, Kakinoki M, et al. Pharmacokinetics of bevacizumab and its effect on vascular endothelial growth factor after intravitreal injection of bevacizumab in macaque eyes. *Invest Ophthalmol Vis Sci.* 2010;51:1606–1608.
10. Zhu Q, Ziemssen F, Henke-Fahle S, et al. Vitreous levels of bevacizumab and vascular endothelial growth factor-A in patients with choroidal neovascularization. *Ophthalmology.* 2008;115:1750–1755.
11. Doft BH, Weiskopf J, Nilsson-Ehle I, Wingard LB Jr. Amphotericin clearance in vitrectomized versus nonvitrectomized eyes. *Ophthalmology.* 1985;92:1601–1605.

12. Chin HS, Park TS, Moon YS, Oh JH. Difference in clearance of intravitreal triamcinolone acetonide between vitrectomized and nonvitrectomized eyes. *Retina*. 2005;25:556–560.
13. Lee SS, Ghosn C, Yu Z, et al. Vitreous VEGF clearance is increased after vitrectomy. *Invest Ophthalmol Vis Sci*. 2010; 51:2135–2138.
14. Yamamoto T, Hitani K, Tsukahara I, et al. Early postoperative retinal thickness changes and complications after vitrectomy for diabetic macular edema. *Am J Ophthalmol*. 2003;135:14–19.
15. Yanyali A, Horozoglu F, Celik E, Nohutcu AF. Long-term outcomes of pars plana vitrectomy with internal limiting membrane removal in diabetic macular edema. *Retina*. 2007; 27:557–566.
16. Hartly KL, Smiddy WE, Flynn HW Jr, Murray TG. Pars plana vitrectomy with internal limiting membrane peeling for diabetic macular edema. *Retina*. 2008;28:410–419.

Clinical Ophthalmology

Dovepress
open access to scientific and medical research

Open Access Full Text Article

CASE REPORT

Analysis of macular cone photoreceptors in a case of occult macular dystrophy

Naoki Tojo
Tomoko Nakamura
Hironori Ozaki
Miyako Oka
Toshihiko Oiwake
Atsushi Hayashi

Department of Ophthalmology, University of Toyama, Toyama, Japan

Purpose: To investigate changes in cone photoreceptors with adaptive optics (AO) fundus imaging and spectral domain optical coherence tomography (SD-OCT) in a case of occult macular dystrophy (OMD).

Patient and methods: Both eyes of a 42-year-old woman diagnosed with OMD were examined. We used an AO fundus camera to obtain images of cone photoreceptors in the macula of the OMD subject and five healthy control subjects. Correlations between the AO images and the SD-OCT images were examined. Cone photoreceptors in eight areas in the macula of OMD and healthy control subjects were analyzed and compared.

Results: SD-OCT showed a loss of the cone outer-segment tips line outside of the fovea in both eyes of the subject with OMD. The left eye with decreased visual acuity showed a discontinuous photoreceptor inner-segment and outer-segment line and cone outer-segment tips line at the fovea in SD-OCT and loss of cone mosaics as a dark spot in the AO image. In panoramic AO images and cone-density maps, less cone density was observed in a ring-like region outside the fovea than in the peripheral retina. In most of the areas examined, the cone densities were lower in the OMD eyes than in the healthy control eyes.

Conclusions: Cone densities in the macula of the OMD patient were greatly decreased. AO images were found to be useful to evaluate morphologic changes in cone photoreceptors in patients with OMD.

Keywords: occult macular dystrophy, adaptive optics, cone photoreceptor, cone analysis, optical coherence tomography

Introduction

Occult macular dystrophy (OMD) is an unusual, inherited macular dystrophy characterized by essentially normal appearances of the fundus and fluorescein angiography, with progressive decrease of visual acuity in both eyes.[1] These patients have normal full-field electroretinograms (ERGs), but show severely decreased macular responses by multifocal ERG.[2] It has been emphasized that the main key to differentiate OMD from other diseases, such as optic neuritis, dominant optic atrophy, amblyopia, or psychological disorders, is the multifocal ERG from the central retina.

Recently, newly developed ophthalmologic instruments have allowed us to investigate the details of retinal morphology in vivo. For example, spectral domain optical coherence tomography (SD-OCT) is a well-established method to examine the layers of retinal architecture.[3] Decreases in foveal thickness and disturbances of the photoreceptor inner- and outer-segment junction (IS/OS) have been observed by SD-OCT in patients with OMD.[4] The adaptive optics (AO) system can compensate

Correspondence: Atsushi Hayashi
Department of Ophthalmology, Graduate School of Medicine and Pharmaceutical Sciences, University of Toyama,
2630 Sugitani, Toyama 930-0194, Japan
Tel +81 76 434 7363
Fax +81 76 434 5037
Email ganka@med.u-toyama.ac.jp

submit your manuscript | www.dovepress.com
Dovepress
http://dx.doi.org/10.2147/OPTH.S44446

for optical aberrations and provide high-resolution retinal images, such as images of cone photoreceptors and retinal vessels.[5] We and others have demonstrated the feasibility of using an AO system to image cone photoreceptors in the macular degeneration of patients.[6–8]

Because the pathophysiology of OMD is not well understood, in the present study we examined correlations between images of SD-OCT and AO in a case with OMD and analyzed cone photoreceptors in the AO images using cone-analysis software.

Methods

The patient underwent complete ophthalmic examinations at Toyama University Hospital, which included a fundus examination, fluorescein angiography, scotopic and photopic full-field ERG, multifocal ERG, SD-OCT, and AO fundus images. Informed consent was obtained after a full explanation of the procedures. All studies were conducted in accordance with the principles embodied in the Declaration of Helsinki. The study protocol for the AO fundus camera was approved by the institutional review board of the University of Toyama.

The diagnosis of OMD was made based on the following findings: normal appearance of the fundus by fundus photography and fluorescein angiography, decreased visual acuity, normal responses of scotopic and photopic full-field ERGs, and reduced amplitudes of multifocal ERG.

The scotopic and photopic full-field ERGs were recorded with an LE-4000 system (Tomey, Nagoya, Japan), and the multifocal ERG was recorded with an LE4100 system (Mayo, Inazawa, Japan), according to the International Society for Clinical Electrophysiology of Vision standards. The stimulus array consisted of 61 hexagons, and the luminance of each hexagon was alternated between 200 cd/m^2 and 5 cd/m^2 with a 75 Hz frame rate. The retinal morphology was investigated by SD-OCT (RS-3000; Nidek, Gamagori, Japan). Fluorescein angiography was performed with an F-10 scanning laser ophthalmoscope (Nidek). After the pupil was dilated with an eye drop of 0.5% toropicamide and 0.5% phenylephrine, AO images of both eyes were taken with an AO fundus camera (RTX1; Imagine Eyes, Orsay, France). The AO images were analyzed with the original cone-analysis software (AODetect; Imagine Eyes) created by the manufacturer.[7] We analyzed the cone density, cone spacing, and mosaic regularity of cone photoreceptors at 500, 1000, 2000, and 3000 mm from the foveal center in the temporal or nasal retina and compared them to the data of healthy control eyes. AO images of five eyes of five healthy control subjects were taken with the RTX1 system and analyzed with the software provided by the manufacturer.

Genetic testing for the retinitis pigmentosa 1-like 1 (*RP1L1*) gene was performed using the blood sample at Nippon Medical School Chiba Hokusoh Hospital as previously described.[9]

Case report

The patient was a 42-year-old woman who did not report a family history of similar visual problems. The best-corrected decimal visual acuity was 1.0 in the right eye and 0.2 in the left eye by a conventional Landolt C chart. Color fundus photographs and fluorescein angiography showed normal findings in both eyes (Figure 1). Multifocal ERG showed reduced amplitudes in the central ring of both eyes (right eye 25.62 nV/deg^2, left eye 11.80 nV/deg^2) (Figure 2A, B, D and E), while scotopic and photopic full-field ERGs showed normal responses (Figure 2C and F). The responses of the central eight areas of multifocal ERG (circles in Figure 2A and D) showed a similar decrease between the nasal and the temporal retina in both eyes. An SD-OCT image revealed a relatively normal IS/OS line and cone outer-segment tips (COST) line at the fovea in the right eye (arrowheads in Figure 3A), with a reduced IS/OS line and unclear COST line in the outside of the fovea (arrows in Figure 3A). A panoramic AO image of the right eye (6.25 × 0.95 mm) showed an extensive loss of cone photoreceptors in the entire area examined, with a ring-like area of residual cone photoreceptors at the fovea (arrowheads in Figure 3B). However, cone photoreceptors were observed at the foveal center (arrow in Figure 3B). An SD-OCT image revealed a discontinuous IS/OS line and COST line at the foveal center in the left eye (asterisk

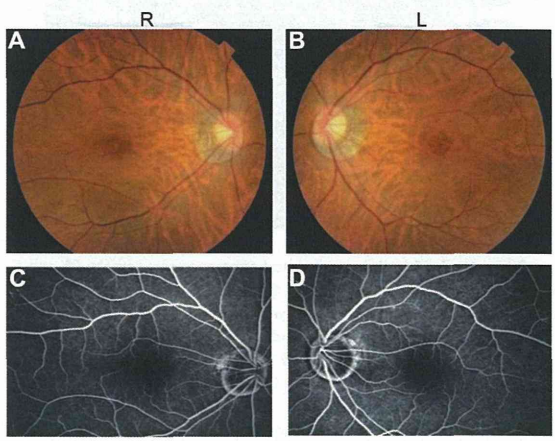

Figure 1 Photographs of the fundus (**A** and **B**) and fluorescein angiography (**C** and **D**) of both eyes of a patient with occult macular dystrophy.
Abbreviations: R, right eye; L, left eye.

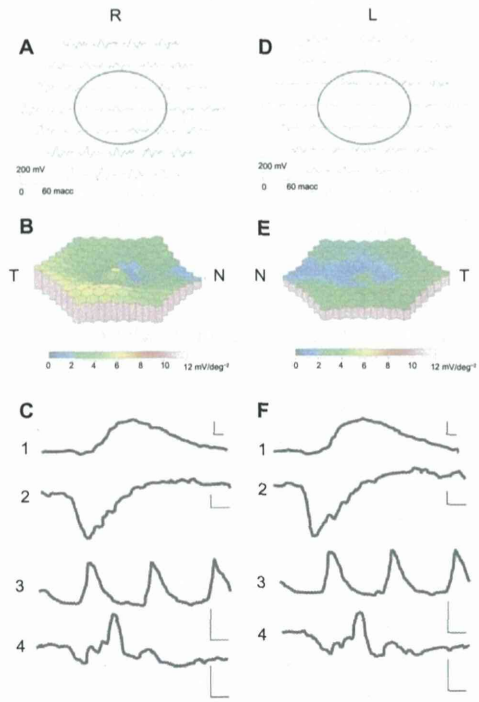

Figure 2 Images of multifocal electroretinograms (ERGs) (**A**, **B**, **D** and **E**), and full-field ERG (**C** and **F**). In the full-field ERG (**C** and **F**), 1 shows the graph for the rod ERG, 2 that for the flash ERG, 3 that for the 30 Hz flicker ERG, and 4 that for the cone ERG.
Note: *The circles of A and D show the response of the central 8 areas. The scales* (C and F) represent 10 ms (horizontal axis) and 100 μV (vertical axis).
Abbreviations: R, right eye; L, left eye; N, nasal; T, temporal.

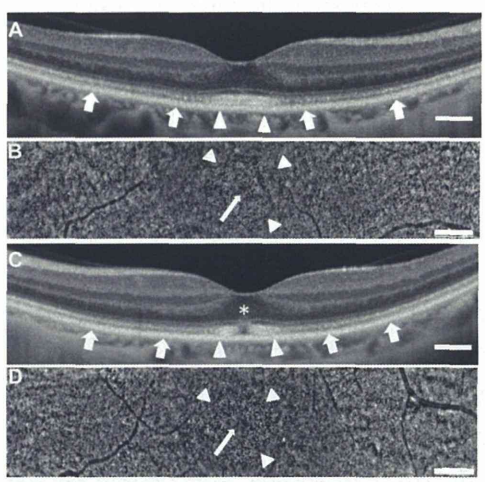

Figure 3 Images of spectral domain optical coherence tomography (**A** and **C**) and adaptive optics (**B** and **D**) at the fovea of the OMD patient.
Notes: Images for the right eye are shown in **A** and **B**, and those for the left eye are presented in **C** and **D**. Panoramic adaptive optics images of **B** the right eye (6.25 × 0.95 mm), and **D** the left eye (6.0 × 1.04 mm). The arrowheads in A and C show areas of observable IS/OS line and COST line at the fovea. The arrowheads in B and D show the corresponding areas in AO images. The long arrow in B and D shows foveal center. The short arrows in A and C show the areas with a reduced IS/OS line and unclear COST line. An asterisk in C shows defect of IS/OS line and COST line. Bar = 500 μm.
Abbreviations: OMD, occult macular dystrophy; IS/OS, inner- and outer-segment; COST, cone outer-segment tips; AO, adaptive optics.

in Figure 3C). Similar to the findings in the right eye, the IS/OS line and the COST line in the left eye were observed at the fovea (arrowheads in Figure 3C), with a reduced IS/OS line and unclear COST line in the outside of the fovea (arrows in Figure 3C). A panoramic AO image of the left eye (6.0 × 1.04 mm) showed an extensive loss of cone photoreceptors in the entire area, with a ring-like region of residual cone photoreceptors at the fovea (arrowheads in Figure 3D). A dark area was observed at the foveal center without cone mosaics (arrow in Figure 3D), and this area corresponded with the area exhibiting loss of the IS/OS line and COST line in the SD-OCT image (asterisk in Figure 3C). The central macular thickness in the SD-OCT images was 148 μm in the right eye and 161 μm in the left eye.

Eight 100 × 100 μm areas at the nasal or temporal retina were selected (avoiding large retinal vessels) in the panoramic AO images (Figure 4A, C and E). The AO images of these areas were analyzed with the software. The distances of nasal (N) 500 and temporal (T) 500, N1000 and T1000, N2000 and T2000, and N3000 and T3000 were 500 μm, 1000 μm, 2000 μm, and 3000 μm from the nasal or temporal foveal center, respectively. The eight areas in a panoramic AO image of a healthy control left eye (6.51 × 0.96 mm) are shown in Figure 4A, and the corresponding cone-density panoramic map is shown in Figure 4B. The results of the cone analysis at these eight areas of the five healthy control eyes are shown in Table 1. The data were expressed as the mean ± standard deviation. As shown in Figure 4B, the cone densities at the foveal center were lower than those at the outside of the foveal center (asterisk in Figure 4B). This was because the resolution of the AO fundus camera was not sufficient to distinguish each cone photoreceptor at the foveal center. Therefore, we did not perform cone analysis at the foveal center in this study.

Both eyes of the OMD case were similarly examined with an AO fundus camera. Eight 100 × 100 μm areas at the nasal or temporal retina were selected (avoiding large retinal vessels) in panoramic AO images of both eyes. A panoramic AO image (6.3 × 1.03 mm) of the right eye is shown in Figure 4C, and the corresponding cone-density panoramic map is shown in Figure 4D. High cone densities were observed at the fovea, while a ring-like area around the fovea showed lower cone densities than the peripheral areas in the nasal or temporal retina (arrowheads in Figure 4D).

A panoramic AO image (6.51 × 0.96 mm) of the left eye is shown in Figure 4E, and the corresponding cone-density panoramic map is shown in Figure 4F. Low cone densities were observed at the foveal center, and these densities corresponded with the dark area of the AO image. The left eye showed a ring-like area of low cone densities around the

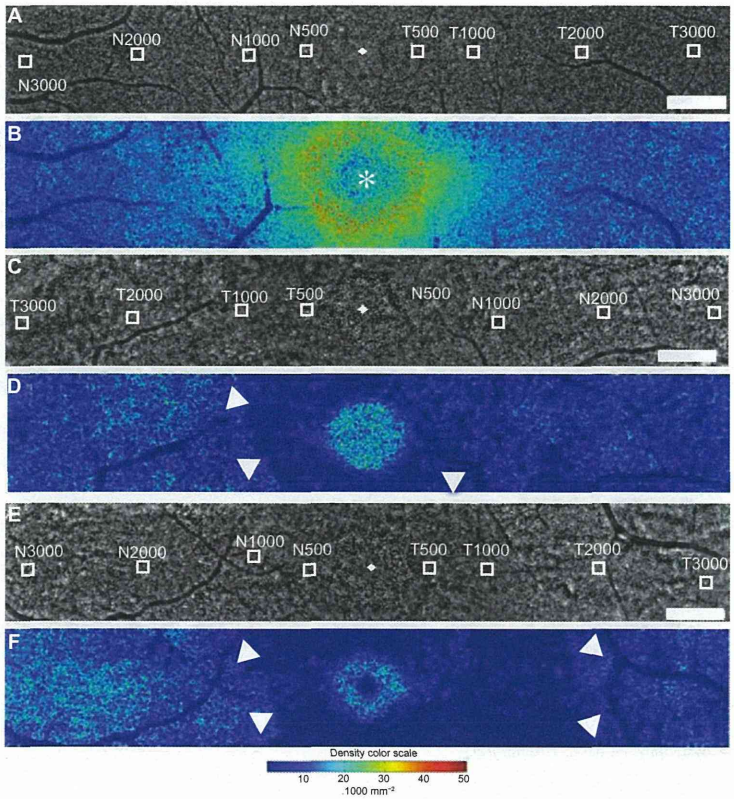

Figure 4 Panoramic adaptive optics images of the left eye of a healthy control (**A**, 6.51 × 0.96 mm), the right eye of the OMD patient (**C**, 6.3 × 1.03 mm), left eye of the OMD patient (**E**, 6.51 × 0.96 mm), and the corresponding cone-density maps (**B**, **D** and **F**), respectively. Eight 100 × 100 μm areas at the nasal or temporal retina were selected (**A**, **C** and **E**).
Notes: The foveal center is indicated by the asterisk in **B**. The arrowheads in D and F show a ring-like dark area around the fovea with lower cone densities than the peripheral areas in the nasal or temporal retina. Bar = 500 μm. A color scale of cone density is shown at the bottom.
Abbreviations: OMD, occult macular dystrophy; N, nasal; T, temporal.

fovea, and this area was similar to, but larger than, that of the right eye (arrowheads in Figure 4F).

Eight areas were analyzed with the software, and the color maps and results are shown in Figure 5A (right eye) and B (left eye) and Table 1. In the right eye, cone densities in the OMD patient were lower than those of the healthy control eyes, except in region N3000. In the left eye, the cone densities of the OMD patient were lower than those of the healthy control eyes, except in regions N2000 and N3000. The cone densities in the temporal retina seemed to be lower

Table 1 Cone analysis of healthy control eyes and both eyes of a patient with OMD

	N500	N1000	N2000	N3000	T500	T1000	T2000	T3000
Density (/mm²)								
Right	3379	6360	10733	9044	1193	3478	3280	6360
Left	2385	5466	15305	14609	2683	1689	6957	5665
Healthy control (n = 5)	25471 ± 3829	18505 ± 2050	14013 ± 1197	10296 ± 2101	25342 ± 2754	20475 ± 1193	14589 ± 1206	11806 ± 2208
Spacing (μm)								
Right	17.62	13.41	10.75	11.64	27.44	117.12	17.5	12.45
Left	25.43	14.79	9.03	8.96	19.7	25.45	12.85	14.83
Healthy control (n = 5)	6.94 ± 0.52	8. 18 ± 0.42	9.32 ± 0.33	10.88 ± 0.98	6.96 ± 0.39	7.81 ± 0.38	9.10 ± 0.39	10.29 ± 0.92
Voronoi (% of six-sided polygons)								
Right	26.5	21.9	44.4	25.3	25.0	22.1	33.3	29.7
Left	33.3	30.9	38.3	31.3	29.6	23.5	28.6	31.6
Healthy control (n = 5)	41.7 ± 4.2	43.9 ± 2.5	40.3 ± 4.1	38.1 ± 4.5	42.6 ± 4.3	51.6 ± 2.6	43.2 ± 6.7	41.6 ± 3.9

Note: Data are means ± standard deviation.
Abbreviations: OMD, occult macular dystrophy; N, nasal; T, temporal.

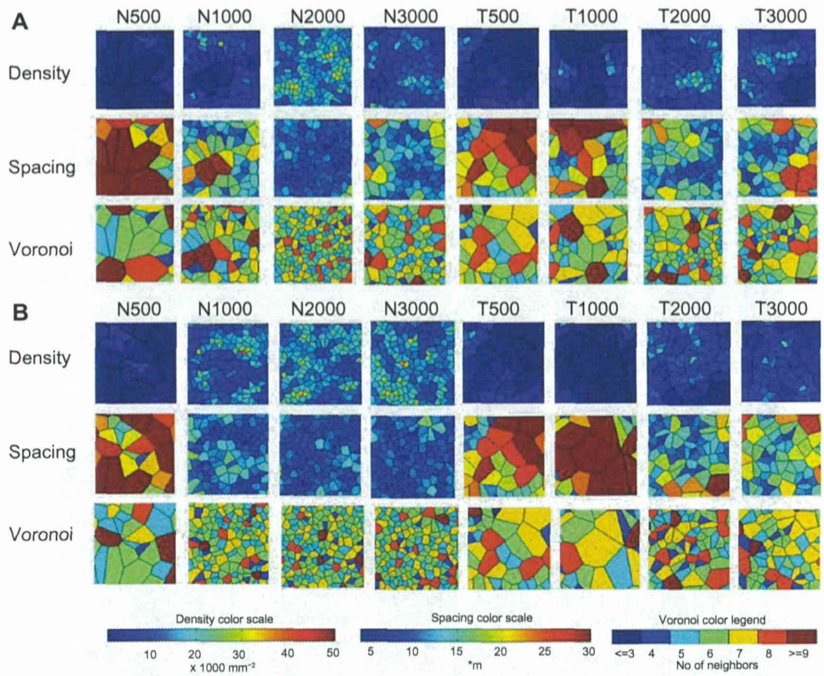

Figure 5 Cone analysis in the eight selected areas of the OMD patient. (**A** right eye, **B** left eye).
Notes: Color maps of cone density, cone spacing, and Voronoi analysis are shown. Color scales for each analysis are shown at the bottom.
Abbreviations: OMD, occult macular dystrophy; N, nasal; T, temporal.

than those in the nasal retina in both eyes. The results of the cone spacing and Voronoi analyses corresponded with those of the cone densities.

In the genetic testing, no mutations in the *RP1L1* gene were detected in this case.

Discussion

OMD is considered to show retinal dysfunctions only in the macula, without apparent changes in ophthalmoscopy and fluorescein angiography.[1,2] Recently, analyses using SD-OCT revealed detailed retinal structures and abnormal changes in patients with OMD.[4,7,10] These findings included thinning of the foveal thickness and the outer nuclear layer,[3] and disruption of the IS/OS line and COST line.[7,10] Park et al reported that photoreceptor disruption sizes in SD-OCT correlated with visual function and disease progression in OMD.[10] We observed similar changes in SD-OCT, but visual function was not analyzed in our case. We also examined the correlations between SD-OCT and AO images, and found that the region with the residual IS/OS line and COST line showed more cone photoreceptors in AO images than did the regions without a COST line.

Since the pathologic changes seemed to be localized in photoreceptors in OMD, investigation of photoreceptors in vivo is important in this disease. For this purpose, examinations with AO systems seemed suitable. Kitaguchi et al reported that patchy dark areas were detected in all examined eyes of patients with OMD.[7] However, detailed cone analyses were not performed in the OMD cases. In this study, we examined AO images of healthy control eyes and both eyes of one OMD case with an AO fundus camera, and cone analyses were performed using the cone-analysis software. In our case, lower cone densities were detected around the fovea than in the peripheral retina examined in both eyes, and the areas in the temporal retina showed particularly reduced cone densities relative to those in the nasal retina. Because cone densities in the temporal retina were shown to be slightly lower within the 1 mm retinal eccentricity than in the nasal retina by histologic and AO studies,[11,12] cone photoreceptors might be more damaged around the fovea and reduced in the temporal retina than in the nasal retina. In addition, the decreased responses in the central eight areas by multifocal ERG correlated with the decrease in cone densities from N3000 to T3000 in the AO images. We could not examine correlations between the cone densities and the amplitudes and implicit times of the ERG responses in the central eight areas, because we examined only one patient with OMD. The examinations of AO images may be useful to monitor changes in cone photoreceptors in OMD cases.

Our case did not show any mutations in the *RP1L1* gene by genetic testing. Because in a previous study, no mutations were detected in four patients with OMD from a single

Caucasian family,[13] OMD is considered to be a genetically heterogeneous disorder.

Because this is a case report, we did not perform any statistical analyses of the cone photoreceptors. However, we demonstrated horizontal distributions of cone mosaics and cone densities of one OMD case with an AO fundus camera. In future studies, it will be necessary to statistically analyze the cone photoreceptors of a greater number of OMD cases using AO systems, and to examine longitudinal changes in the cone photoreceptors and correlations between cone analyses and other fundus-imaging findings.

Acknowledgment

The authors are deeply grateful to Shuhei Kameya, MD, PhD, of Nippon Medical School Chiba Hokusoh Hospital, Chiba, Japan, for performing the genetic testing.

Disclosure

The authors report no conflicts of interest in this work.

References

1. Miyake Y, Ichikawa K, Shiose Y, Kawase Y. Hereditary macular dystrophy without visible fundus abnormality. *Am J Ophthalmol*. 1989;108:292–299.
2. Miyake Y, Horiguchi M, Tomita N, et al. Occult macular dystrophy. *Am J Ophthalmol*. 1996;122:644–653.
3. Ooto S, Hangai M, Tomidokoro A, et al. Effects of age, sex, and axial length on the three-dimensional profile of normal macular layer structures. *Invest Ophthalmol Vis Sci*. 2011;52:8769–8779.
4. Brockhurst RJ, Sandberg MA. Optical coherence tomography findings in occult macular dystrophy. *Am J Ophthalmol*. 2007;143:516–518.
5. Williams DR. Imaging single cells in the living retina. *Vision Res*. 2011;51:1379–1396.
6. Duncan JL, Zhang Y, Gandhi J. High-resolution imaging with adaptive optics in patients with inherited retinal degeneration. *Invest Ophthalmol Vis Sci*. 2007;48:3283–3291.
7. Kitaguchi Y, Kusaka S, Yamaguchi T, Mihashi T, Fujikado T. Detection of photoreceptor disruption by adaptive optics fundus imaging and Fourier-domain optical coherence tomography in eyes with occult macular dystrophy. *Clin Ophthalmol*. 2011;5:345–351.
8. Tojo N, Nakamura T, Fuchizawa C, Oiwake T, Hayashi A. Adaptive optics fundus images of cone photoreceptors in the macula of patients with retinitis pigmentosa. *Clin Ophthalmol*. 2013;7:203–210.
9. Akahori M, Tsunoda K, Miyake Y, et al. Dominant mutations in RP1L1 are responsible for occult macular dystrophy. *Am J Hum Genet*. 2010;87:424–429.
10. Park SJ, Woo SJ, Park KH, Hwang JM, Chung H. Morphologic photoreceptor abnormality in occult macular dystrophy on spectral-domain optical coherence tomography. *Invest Ophthalmol Vis Sci*. 2010;51:3673–3679.
11. Curcio CA, Sloan KR, Kalina RE, Hendrickson AE. Human photoreceptor topography. *J Comp Neurol*. 1990;292:497–523.
12. Song H, Chui TY, Zhong Z, Elsner AE, Burns SA. Variation of cone photoreceptor packing density with retinal eccentricity and age. *Invest Ophthalmol Vis Sci*. 2011;52:7376–7384.
13. Chen CJ, Scholl HPN, Birch DG, Iwata T, Miller NR, Goldberg MF. Characterizing the phenotype and genotype of a family with occult macular dystrophy. *Arch Ophthalmol*. 2012;130:1554–1559.

Vitrectomy without Laser Treatment or Gas Tamponade for Macular Detachment Associated with an Optic Disc Pit

Akito Hirakata, MD,[1] Makoto Inoue, MD,[1] Tomoyuki Hiraoka, MD,[1] Brooks W. McCuen II, MD[2]

Purpose: To evaluate the clinical outcomes after vitrectomy, without gas tamponade or laser photocoagulation to the margin of the optic nerve, for the treatment of macular detachment associated with optic disc pits and to characterize retinal manifestations during treatment of optic pit maculopathy using optical coherence tomography (OCT).

Design: Noncomparative, retrospective, interventional case series.

Participants: Eight consecutive patients (8 to 56 years of age) with unilateral macular detachment associated with optic disc pit.

Intervention: Pars plana vitrectomy with induction of a posterior vitreous detachment (PVD) was performed in all eyes. No laser or gas injection was performed in any eye during the original surgery. Patients were followed up for 10 to 46 months (mean, 26 months) after surgery.

Main Outcome Measures: Anatomic outcome as determined by OCT and postoperative visual acuities were the main outcome parameters. Fundus autofluorescence (FAF) images were obtained in 4 eyes to document anatomic changes in the macula.

Results: Although complete retinal reattachment was achieved in 7 of 8 eyes, up to about 1 year was necessary for the retinal detachment to resolve fully. The 1 eye in which macular detachment failed to resolve completely underwent revision of vitrectomy with a gas tamponade and laser photocoagulation in the peripapillary area. In the early postoperative period, despite persistent macular detachment, the visual acuities improved in 7 eyes. These improved acuities corresponded with remodeling of the photoreceptor outer segments on OCT and the appearance of granular hyperfluorescence on FAF imaging.

Conclusions: Vitrectomy with induction of a PVD at the optic disc without gas tamponade or laser photocoagulation seems to be an effective method of managing macular detachment resulting from optic disc pits. The OCT scanning before and after surgery suggests that peripapillary vitreous traction with the passage of fluid into the retina through the pit is the cause of the schisis-like separation seen in optic disc pit maculopathy.

Financial Disclosure(s): The author(s) have no proprietary or commercial interest in any materials discussed in this article. *Ophthalmology 2012;119:810–818 © 2012 by the American Academy of Ophthalmology.*

An optic disc pit is a congenital anomaly of the optic nerve frequently associated with macular detachment.[1–4] Optical coherence tomography (OCT) has confirmed the observation of Lincoff et al[5] that there was frequently a retinoschisis-like separation of the retina present during the development of serous macular detachment.[6–8] However, the pathogenesis of optic disc pit maculopathy remains unclear.

The treatment of optic disc pit maculopathy remains controversial. The use of peripapillary laser therapy to produce a barrier of chorioretinal adhesions at the optic disc border with or without intravitreous gas injection often is unsuccessful, and repeated treatments are needed.[9–13] Although Theodossiadis[14] reported that macular scleral buckling can yield favorable anatomic and functional results, this techniques has not been adopted widely. Lincoff et al[15] reported that intravitreal gas injection alone can induce pneumatic displacement of the outer layer detachment and can improve central vision. However, this beneficial effect may be only temporary, because recurrence of macular involvement caused by fluid movement into the subretinal space from persistent inner layer separation has been shown by OCT.[8]

The authors previously reported that the induction of posterior vitreous detachment (PVD) and gas tamponade without laser treatment for optic disc pit maculopathy is effective in reattaching the retina and improving visual acuity.[16] This finding suggested that vitreous traction around the optic disc pit may cause passive fluid migration into the intraretinal space through the pit. Although the ultimate success rate in this series was high, most eyes required almost 1 year to reach complete reattachment after vitrectomy and gas tamponade. Because of the long time necessary for resolution of the subretinal fluid in this series, the authors hypothesized that the gas tamponade may not be necessary for success. Not performing a gas tamponade in these cases allows elimination of the need for prone positioning after surgery, as well as any complications related to fluid–air exchange or gas tamponade. In addition, the early postoperative events are studied better with OCT in the fluid-filled eye compared with the gas-filled eye. The pur-

ISSN 0161-6420/12/$–see front matter
doi:10.1016/j.ophtha.2011.09.026

pose of this study was to evaluate the clinical outcomes in 8 consecutive eyes that underwent vitrectomy with PVD induction without gas tamponade or laser application for the treatment of optic disc pit maculopathy and to characterize the course of retinal reattachment after surgery for optic disc pit maculopathy.

Patients and Methods

Eight eyes of 8 consecutive patients with optic disc pit maculopathy who sought treatment at the Kyorin Eye Center or Duke Eye Center were included in this study. This study had Kyorin University or Duke University Institutional Review Board approval and records were reviewed retrospectively. This clinical study has been registered at the United States National Institutes of Health (www.clinicaltrials.gov) as "Vitrectomy for Optic Disc Pit Maculopathy" with a reference number of NCT01340703. Best-corrected visual acuity (BCVA) was recorded and indirect funduscopy and slit-lamp biomicroscopy using a 90-diopter noncontact lens were performed before and after surgery. The OCT images of the eyes were obtained using Stratus OCT (Carl Zeiss Meditec, Inc., Dublin, CA), OCT 4000 Cirrus (Carl Zeiss Meditec, Inc.), or Spectralis OCT (Heidelberg Engineering, Heidelberg, Germany) to evaluate posterior retinal changes during follow-up. The fundus autofluorescence (FAF) images obtained by confocal scanning laser ophthalmoscopy (cSLO) (Heidelberg Retina Angiograph 2; Heidelberg Engineering) also were evaluated and compared with the ophthalmologic and OCT images beginning in 2009.

Surgery was performed for worsening BCVA or for the development of macular detachment. Surgeries were performed by 3 surgeons (A.H., M.I., or B.W.M.) between 2005 and 2009, and patients were followed up for 10 to 46 months after surgery (mean, 26 months). Vitrectomy was performed with the intention of releasing vitreous traction at the optic disc pit. Twenty-gauge vitrectomy was performed in 3 eyes and 25-gauge vitrectomy was performed in 5 eyes. Posterior vitreous detachment was initiated by suction over the optic disc or near areas of retinoschisis-like separation using the vitreous cutter or microhook. To limit retinal damage secondary to surgical manipulation, special attention was given to separating the posterior hyaloid gently over schisis-like areas. Triamcinolone acetonide was used during surgery to visualize better the posterior cortical vitreous.[17] The internal limiting membrane (ILM) was removed after PVD induction in one patient (patient 8) because the ILM in this patient was separated from the surface of retina before surgery. Neither a gas tamponade nor laser photocoagulation was performed during the primary procedure in any of these cases.

Results

Preoperative Clinical Characteristics

The clinical characteristics of all 8 patients are shown in Table 1, and clinical photographs of representative patients are shown in Figures 1, 2, and 3. Six of the patients were male and 2 were female, with ages ranging from 8 to 56 years (mean, 32.3 years). All patients were of Japanese ethnicity except for patient 3, who was white. All patients reported decreased BCVA, a central scotoma, or metamorphopsia in the affected eye for more than several months. Seven of the affected eyes had no significant refractive error and 1 eye (patient 4) had moderate myopia. The preoperative Snellen BCVA ranged from 20/300 to 20/20 (mean, 20/67). One patient had a chorioretinal coloboma below the optic disc in addition to the optic disc pit (patient 4). No patients had undergone any prior treatment for their optic disc pit maculopathy. The younger two patients (patients 2 and 7) noted their visual disturbance after blunt ocular trauma, when a macular detachment associated with an optic disc pit was diagnosed in the eye. One patient (patient 6) had a medical history of central serous chorioretinopathy treated with laser approximately 20 years previously in the affected eye, but no visible laser scar was apparent. The other 5 patients had no pertinent medical or ocular history.

The presence of a schisis-like separation was confirmed before surgery in 7 of 8 eyes. One patient (patient 3) had macular detachment only. An outer layer schisis-like separation was found in 6 eyes, and multiple shallow inner layer schisis-like separations (edema-like spaces) with or without ILM separation were noted in 5 eyes. Macular retinal detachment (RD) initially was observed in 7 of 8 eyes. This RD did not connect to the optic disc in 5 eyes, but was connected in 2 eyes (patients 3 and 7). Patient 8 had multiple layers of retinal separation, including marked separation of the ILM, but no apparent RD. This patient initially sought treatment with a BCVA of 20/20 and reporting metamorphopsia. One month later, a macular detachment developed with a decrease in the BCVA (Fig 3). The OCT images could not detect any definite communication between the schisis-like separation and vitreous cavity in any of the eyes. Neither PVD nor vitreomacular traction was observed in any of the eyes before surgery by fundus biomicroscopy or OCT scanning.

Anatomic Results

Complete retinal reattachment as determined by OCT images was achieved in 7 of 8 eyes after initial treatment (Figs 1 and 2). No recurrences were observed in these 7 eyes. The other eye (patient 6) showed an initial reduction in the height of the macular detachment with improved BCVA and decreased metamorphopsia over the first few postoperative months, but increased macular elevation developed approximately 10 months after surgery, with the BCVA dropping to 20/200 (Fig 3). An intravitreal gas injection was performed with postoperative prone positioning, but the detachment failed to improve. The patient then underwent revision of vitrectomy with ILM peeling over posterior pole, subretinal fluid drainage, and placement of a gas tamponade. After surgery, submacular fluid with a shallow retinoschisis-like separation recurred. The OCT scans obtained during the recurrence of subretinal fluid showed a relatively high elevation of the retina around a vessel at the margin of the optic disc, leading to application of laser photocoagulation to a small area beside the vessel in the peripapillary region (only 6 laser spots). At 4 months after photocoagulation, the area of RD had shifted superiorly and appeared smaller. The OCT imaging in the peripapillary area revealed a communication between the subretinal fluid and the perivascular area near the optic disc pit (Fig 3). Seven months after photocoagulation, the retinal detachment had resolved, corresponding to an increase in hyperfluorescence on FAF imaging (Fig 3).

Postoperative OCT scanning in the 7 successful eyes demonstrated that the sharp contour of retinal elevation adjacent to the optic disc and inner retinoschisis-like separation (edema-like spaces) were reduced immediately, whereas in most eyes, the outer retinoschisis-like separation decreased slowly after vitrectomy. After reduction of the retinoschisis-like separation, the macular detachment decreased gradually with complete absorption of fluid after 6 to 16 months (average, 12 months; Figs 1 and 2). As the RD slowly resolved, there was an increase in the amount of subretinal precipitates; this corresponded to a thickening of the photoreceptor outer segments (Figs 1 and 2). A limited defect in the outer segments of photoreceptors or the inner segment/outer segment line at the fovea remained even after persistent complete retinal

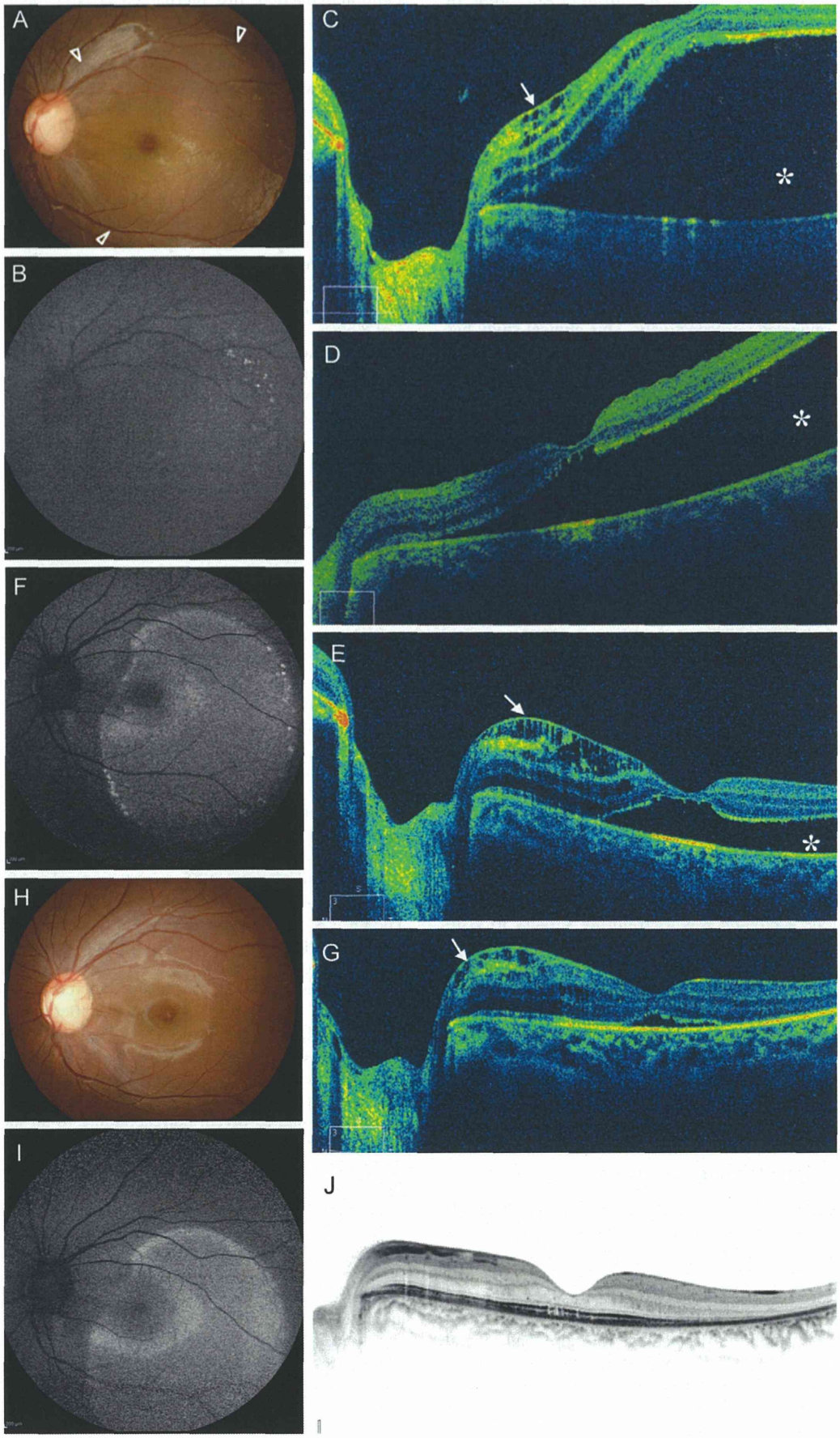
A
B
C
D
E
F
G
H
I
J